IEEJ Journal of Industry Applications
Vol.7 No.4 pp.298–304 DOI: 10.1541/ieejjia.7.298

Paper

Iron Loss and Hysteretic Properties under PWM Inverter Excitation at High Ambient Temperatures

Atsushi Yao[*,**a)] Member, Shunya Odawara[***] Member
Keisuke Fujisaki[*] Senior Member

(Manuscript received Sep. 27, 2017, revised Jan. 18, 2018)

We experimentally and numerically investigate the magnetic properties of magnetic materials excited by sinusoidal and pulse width modulation (PWM) inverter input at high ambient and room temperatures. We show that the iron losses under sinusoidal and PWM inverter excitations decrease with an increase in temperature. It is found that the temperature dependency of iron loss properties is related not only to major loop but also to minor loops. Furthermore, we derive the numerical expression for the hysteretic properties of the PWM inverter- and sinusoidal-fed ring tests at room temperature and 300°C by using the play model with the Cauer circuit.

Keywords: inverter, iron loss, high-temperatures, play model, Cauer circuit

1. Introduction

Several researchers have recently addressed high-temperature motor drive system in harsh temperature environments like aerospace, automotive, and fire sites [(1)(2)]. In such high-temperature motor drive system, to control the rotational speed and electromagnetic torque of electrical motors, pulse width modulation (PWM) inverters [(3)] are often used. Many studies have shown that iron losses of soft magnetic materials (used as a motor core) are very different whether it is fed by sinusoidal or PWM inverter inputs at room temperature [(4)–(11)]. In addition, some researchers have recently demonstrated changes of magnetic properties under sinusoidal excitation at high temperatures [(12)–(15)]. Therefore, in order to realize high temperature and high efficiency motor drive system, the next step is to correctly understand magnetic properties of PWM inverter-fed magnetic materials under a wide range of ambient temperatures. The goal of the work presented in this paper is to experimentally and numerically examine iron loss properties and hysteretic properties of magnetic materials under sinusoidal and PWM inverter excitations at high temperatures.

Recently, considerable attention has been paid to describing hysteretic phenomena by numerical simulations [(16)–(24)]. In order to achieve the highly accurate power electronics (*e.g.* motor drive system) simulation, it is necessary to numerically represent the magnetic hysteretic properties of soft magnetic materials. However, it is difficult to accurately express hysteretic properties by numerical simulations because of the complexity of physical phenomena and computational costs. To solve these problems, for the nonlinear hysteretic properties modeling at room temperature, the play model [(16)–(18)] with the Cauer circuit [(19)–(21)] has been studied because its physical meaning is clear [(22)(23)]. This paper attempts to apply the play model with the Cauer circuit to represent the magnetic hysteretic properties of magnetic materials under sinusoidal and PWM inverter excitations at high temperatures.

In this study, we experimentally and numerically address magnetic properties of magnetic materials excited by sinusoidal and PWM inverter input under a wide range of ambient temperatures. We experimentally examine the iron loss characteristics and hysteretic properties of a ring specimen made of magnetic materials at room temperature and 300°C. In addition, in order to represent the magnetic hysteretic properties at high temperatures, the play model with the Cauer circuit is used for the numerical simulations. The authors have published papers [(25)(26)] in conferences to discuss a part of the experimental results of this work. This paper is an improved version of those papers.

2. Measurement System

Figure 1 shows the configuration of the experimental setup used to measure the iron loss characteristics of a ring specimen under a wide range of ambient temperatures. In our study, the ring specimen is composed of laminations of standard non-oriented electrical (NO) steel sheets [(11)] and is exposed to ambient temperature variations in the oven to evaluate temperature dependency of iron loss properties. Table 1 shows the characteristics of the ring specimen and its material. By using this experimental system, we perform two kinds of excitation tests under a wide range of temperatures. The first ring test is carried out under sinusoidal excitation by using a function generator (FGX-295, TEXIO) and a linear

a) Correspondence to: Atsushi Yao. E-mail: yao@pu-toyama.ac.jp
* Department of Advanced Science and Technology, Toyota Technological Institute
2-12-1, Hisakata, Tenpaku-ku, Nagoya 468-8511, Japan
** Department of Electrical and Computer Engineering, Toyama Prefectural University
5180, Kurokawa, Imizu 939-0398, Japan
*** Department of Electrical and Electronic Engineering, Kitami Institute of Technology
165, Koencho, Kitami 090-8507, Japan

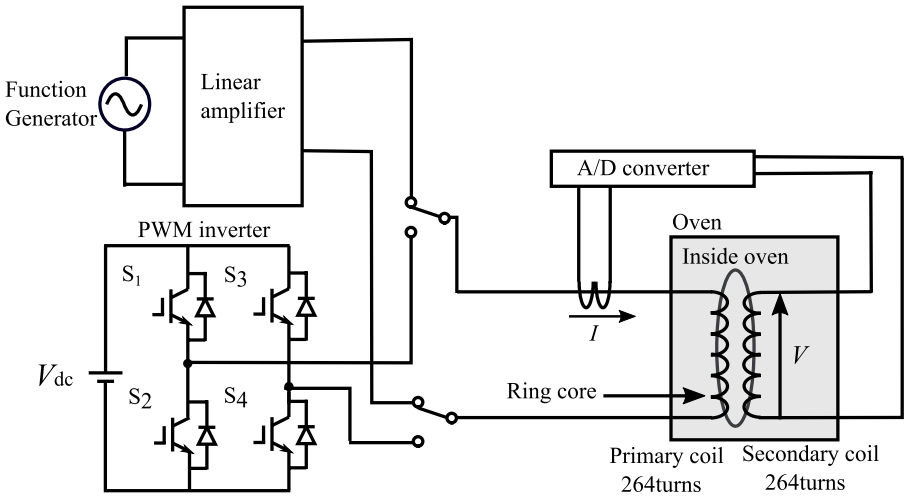

Fig. 1. Schematic of ring tests to experimentally obtain the iron losses properties under a wide range of temperature. The ring specimen is excited by PWM inverter or sinusoidal inputs

Table 1. Specifications of ring specimen and its material

Characteristic	Symbol	Value
Material		35H300
Height	d	7 mm
Density	ρ	7650 kg/m^3
Average magnetic path length	l	0.36 m
Cross section area	S	87.5 mm^2
Primary coil winding	N_1	264 turns
Secondary coil winding	N_2	264 turns

amplifier (HSA 4014, NF) with a frequency of 50 Hz. The second test is to measure the ring core excited by a PWM inverter signal using a single phase PWM inverter (MWINV-9r122B, Myway) that has a fundamental frequency f_0 and a carrier frequency f_c.

In order to evaluate the iron loss characteristics of the ring specimen under a wide range of temperatures, we measure the magnetic field intensity H and the magnetic flux density B. To obtain H and B, this ring specimen consists of two coils wound with round wire; The primary and secondary coils are used as an exciting coil and a B-coil wound, respectively. The current I flowing in the primary coil of the ring specimen is measured and then the magnetic field intensity H is given by

$$H = \frac{N_1 I}{l}, \quad \cdots\cdots (1)$$

where N_1 denotes the number of turns of the exciting coil and l is the magnetic path length. In our experiments, the B-coil voltage V is measured using the B-coil wound around the ring specimen and then the magnetic flux density B is given by

$$B = \frac{1}{N_2 S}\int V dt, \quad \cdots\cdots (2)$$

where N_2 denotes the number of turns of B-coil and S is the cross section area of the ring.

By integrating H and B, the iron losses W_{ring} of the ring specimen is obtained as

$$W_{\text{ring}} = \frac{f_0}{\rho}\int H\mathrm{d}B, \quad \cdots\cdots (3)$$

where ρ is the density of the magnetic sheet.

In our study, the rate of increase of iron loss η is defined by

$$\eta = \frac{W_{\text{ring}}^{\text{INV}}}{W_{\text{ring}}^{\text{SIN}}}, \quad \cdots\cdots (4)$$

where $W_{\text{ring}}^{\text{INV}}$ and $W_{\text{ring}}^{\text{SIN}}$ are the iron losses under PWM inverter and sinusoidal excitations, respectively. Note that, for the calculation, $W_{\text{ring}}^{\text{INV}}$ and $W_{\text{ring}}^{\text{SIN}}$ depend on temperatures.

3. Numerical Simulation Method

We consider to express magnetic hysteretic properties of NO steel sheets under a wide range of ambient temperatures by numerical simulations. To do this, we employ the dynamic hysteresis model that combines the play model with the Cauer circuit [22][23]. Roughly speaking, in our simulations, the play model expresses numerical DC magnetic hysteresis loop based on experimental DC hysteresis loops at each temperature, as shown in Fig. 2, and the Cauer circuit with two inductors shown in Fig. 3 represents AC components of hysteresis loops (See Refs. (22), (23) for details of the play model with the Cauer circuit at room temperature.). In the Cauer circuit, the terminal voltage V, the terminal current I, and the inductance L correspond to $\mathrm{d}B/\mathrm{d}t$, H, and the magnetic permeability μ, respectively. Therefore, in the play model with the Cauer circuit, the hysteresis loop is described by

$$H_{\text{AC}}(B) = \frac{B^k}{L} + \frac{7(B^k - B^{k-1}) + 2L'h_2^{k-1}}{7R_{\text{E}}\Delta t + 2L'} + \frac{3L'(h_2^k - h_2^{k-1})}{35R_{\text{E}}\Delta t}, \quad \cdots\cdots (5)$$

$$= H_{\text{DC}}(B) + \frac{7(B^k - B^{k-1}) + 2L'h_2^{k-1}}{7R_{\text{E}}\Delta t + 2L'} + \frac{3L'(h_2^k - h_2^{k-1})}{35R_{\text{E}}\Delta t}, \quad \cdots\cdots (6)$$

$$R_{\text{E}} = \frac{12}{\alpha\sigma d^2}, \quad \cdots\cdots (7)$$

where $H_{\text{DC}}(B)$ denotes the static (DC) hysteretic property represented by the play model, Δt is the time division, d is the thickness of steel sheet, σ is the electrical conductivity of steel sheet, R_E is the resistance to represent eddy currents and k is the step number. α and L' are fitting

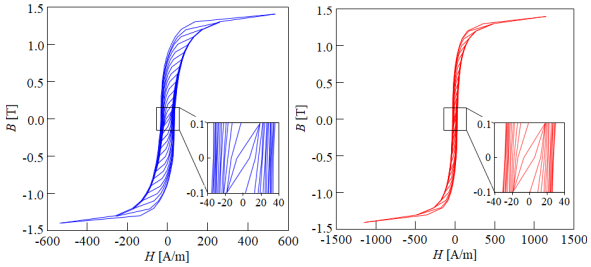

Fig. 2. DC hysteresis loops (experimental results): These loops are used as input of numerical simulations of Eq. (6): (a) Results at room temperature. (b) Loops at 300°C

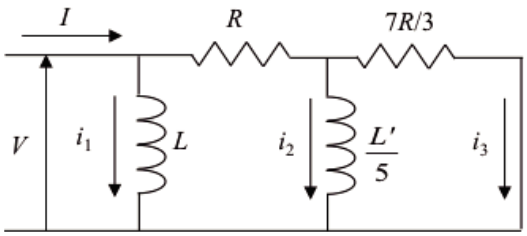

Fig. 3. Cauer circuit of resistive termination

parameters corresponding to the anomaly factor to express anomaly eddy currents and corresponding to the equivalent inductance to express the magnetic flux caused by eddy currents, respectively.

In our study, σ at room temperature and 300°C are set to 1.923×10^6 and 1.354×10^6 S/m, respectively, based on Refs. (27) and (28). Thus, the electrical resistivity is 0.5200 and 0.7386 $\mu\Omega$·m at room temperature and 300°C, respectively. The electrical resistivity at 300°C is about 1.42 times of that at room temperature. In the following simulations, L' under sinusoidal excitation is fixed at 0 because the hysteretic properties of the sinusoidal-fed ring specimen are mostly not influenced by the magnetic flux caused by eddy currents [22]. Based on the experimental results, the magnetic flux density B input for Eq. (6) is generated by ideal sinusoidal or PWM voltage waveforms.

4. Results and Discussion

4.1 Sinusoidal Excitation Figure 4(a) shows the experimentally determined hysteresis loops of the sinusoidal-excited ring at room temperature and 300°C. The peak magnetic flux density in the ring core is set to 1 T by tuning the applied voltage. The iron losses of the ring specimen under sinusoidal excitation are about 1.02 W/kg and 0.86 W/kg at room temperature and 300°C, respectively. The iron loss under sinusoidal excitation decreases with the increase of temperature.

Figure 4(b) shows the hysteresis loops obtained numerically by the play model with the Cauer circuit at room temperature and 300°C. We fit the iron losses under sinusoidal excitation with Eq. (6), where α is a fitting parameter corresponding to the anomaly factor. Here, in order to equalize the numerical iron loss to the experimental iron loss, α is swept and adjusted to 2.14 and 2.55 at room temperature and 300°C, respectively. The calculated iron losses are quantitatively consistent with the experimental iron losses. The numerical

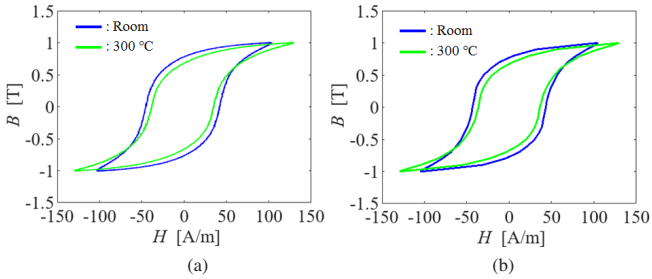

Fig. 4. Hysteresis loops under sinusoidal excitation at room temperature and 300°C: (a) Experimental results. (b) Corresponding numerical loops

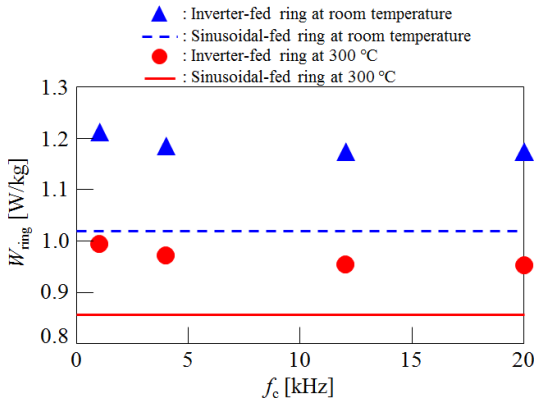

Fig. 5. Experimentally obtained iron losses of ring specimen as a function of carrier frequency at $f_0 = 50$ Hz and $B = 1$ T. Tests are performed at carrier frequencies f_c of 1, 4, 12, and 20 kHz. The iron losses is calculated by integrating H and B with Eq. (3)

simulation well expresses the hysteresis loops. Therefore, we realize the expression of hysteretic properties under sinusoidal excitation at wide range of temperature by numerical simulations.

It is well known that the classical eddy current loss is inversely proportional to the electrical resistivity [29][30]. As mentioned above, the electrical resistivity at 300°C is larger than that at room temperature. Therefore, it is thought that the classical eddy current loss decreases with the increase of electrical resistivity at high temperatures. As shown in Fig. 2, the coercivity at 300°C is smaller than that at room temperature because it is considered that there appears thermal fluctuation at high temperatures. Here, the area of DC hysteresis loop corresponds to the hysteresis loss. Therefore, it is thought that the hysteresis loss decreases [15] due to thermal fluctuation at high temperatures. It is thought that the total iron loss (eddy current and hysteresis losses) under sinusoidal excitation decreases with the increase of temperature because the classical eddy current loss decreases with the increase of electrical resistivity and the hysteresis loss decreases due to thermal fluctuation at high temperatures. The ratio between hysteresis and eddy current losses will be examined at room and high temperatures in the near future.

4.2 Inverter Excitation Figure 5 shows the experimentally obtained iron losses of the ring specimen under PWM inverter excitation at room temperature and 300°C. In other words, blue and red dots correspond to iron losses for whole $B - H$ locus including the locus of the minor loop

(shown in the below figures). The figure also shows the iron loss of the ring specimen under sinusoidal excitation for comparison purposes. The fundamental frequency, the switching dead-time, and the modulation index are set to 50 Hz, 3500 ns, and 0.7, respectively. In our study, four carrier frequencies (1, 4, 12, and 20 kHz) are evaluated. The applied voltage V_{dc} in the inverter test is adjusted to obtain the maximum magnetic flux density of 1 T as in the sinusoidal test. The iron loss under PWM inverter excitation decreases with increasing temperatures.

Figure 6 shows the rate of increase of the iron loss η obtained from Eq. (4). The squares (circles) correspond to η calculated from the iron losses under inverter and sinusoidal excitations at room temperature (at 300°C). Note that η at 300°C becomes small in comparison with that at room temperature. In order to discuss the reasons for the change of η, the magnetic hysteresis properties are investigated.

The thin (green) lines in Fig. 7 show experimental hysteresis loops under PWM inverter excitation at room temperature and 300°C. The hysteresis loops have a major loop and a lot of minor loops. Here, as shown in Fig. 7(a), the

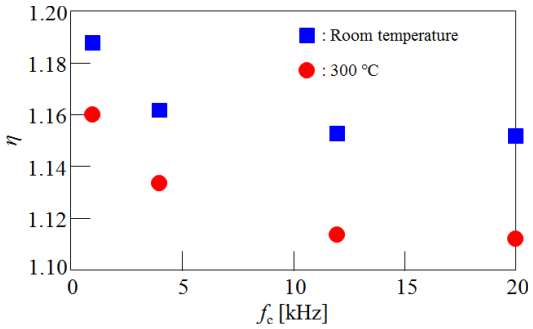

Fig. 6. Experimentally determined rate of increase of iron loss η at room temperature and 300°C. η is obtained from Eq. (4)

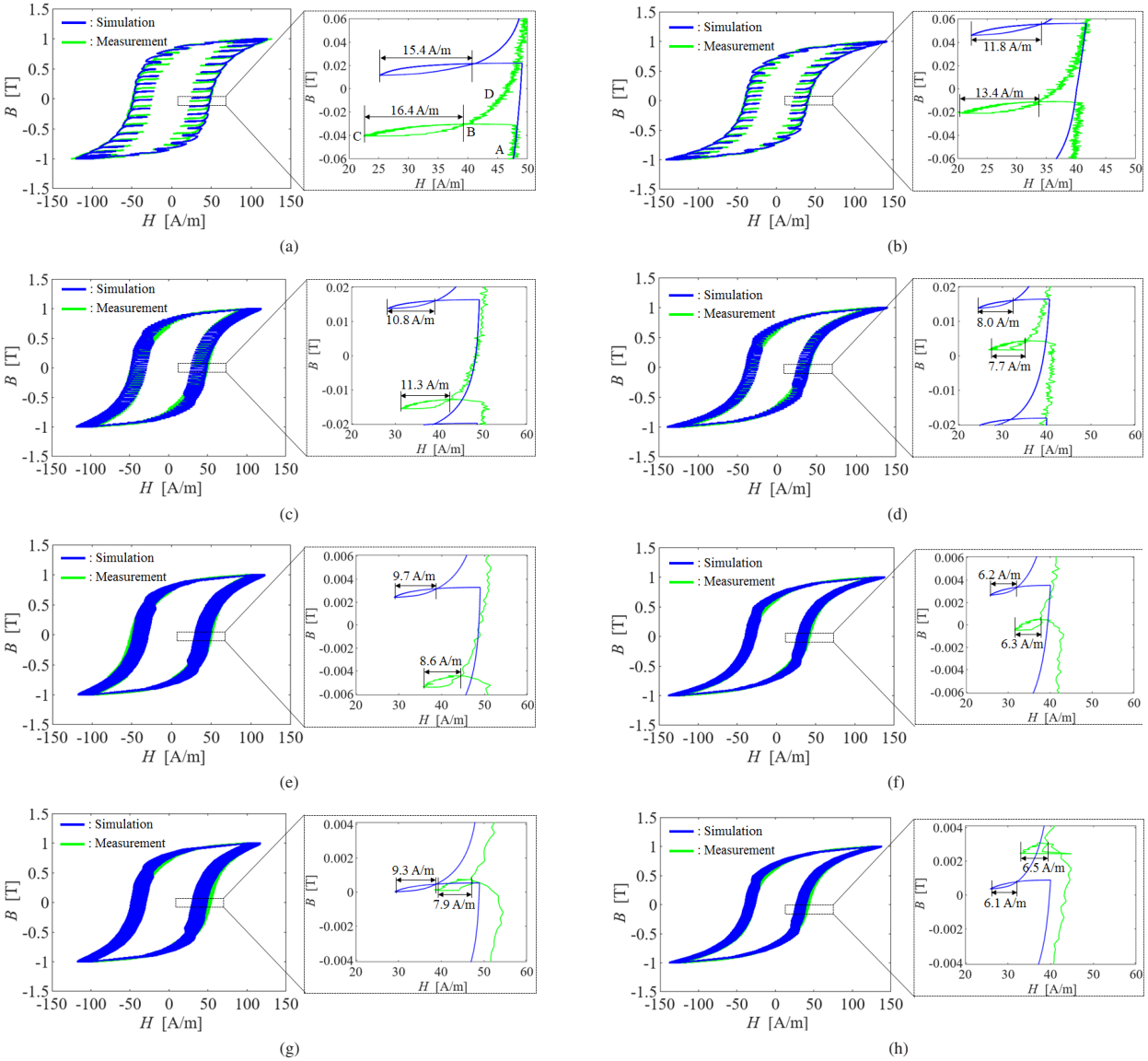

Fig. 7. Experimentally and numerically obtained hysteresis loops of NO ring excited by PWM inverter at room temperature and 300°C. The thin (green) and dark (blue) lines correspond to experimental and numerical loops, respectively. The magnified figures show minor loops of hysteresis loops: (a) f_c = 1 kHz and room temperature. (b) f_c = 1 kHz and 300°C. (c) f_c = 4 kHz and room temperature. (d) f_c = 4 kHz and 300°C. (e) f_c = 12 kHz and room temperature. (f) f_c = 12 kHz and 300°C. (g) f_c = 20 kHz and room temperature. (h) f_c = 20 kHz and 300°C

hysteresis loop under inverter excitation makes a trace of A→B→C→B→D. Then, the trace of B→C→B is defined as one of the minor loops that have a point of intersection in the major loop (See Ref. (7) for details of the major and minor loops.). When the minor loops appear in the hysteresis loops, the area of hysteresis loops becomes large [7]. Therefore, due to the minor loops, the input supplied by the PWM inverter increases iron losses (the area of hysteresis loops) compared to the sinusoidal input [7]. See Appendix 1 for the details of waveforms of the induced voltage and magnetic flux density corresponding to the minor loop.

Figure 7 also shows the numerical results under PWM inverter excitation at f_c = 1, 4, 12, and 20 kHz. The numerical iron losses are fit to the measured iron losses, thereby obtaining L' = 3.3, 1.4, 0.51, and 0.32 mH (L' = 5.4, 2.2, 1.0, and 0.64 mH) at room temperature (300°C) and at f_c = 1, 4, 12, and 20 kHz, as the numerically adjusted parameter. Here, in order to equalize the numerical iron loss to the experimental iron loss, L' is swept and adjusted at room temperature and 300°C. Here, we numerically demonstrate the representation of the hysteretic phenomena of soft magnetic materials under PWM inverter excitation at room temperature and 300°C. In particular, the minor loop of the magnetic hysteretic properties can be expressed numerically by the play model with the Cauer circuit at high temperatures, as shown in the magnified figures.

The Cauer circuit with two inductors used in our study can well express the skin effect up to 40 kHz [31]. Here, the minor loops at high carrier frequency shown in Figs. 7(g) and (h) depend more on higher harmonic components of more than 40 kHz compared to minor loops at low carrier frequency shown in Figs. 7(a)–(f). Therefore, the difference between experimental and numerical loops (major and minor loops) shown in Figs. 7(g) and (h) becomes slightly large in comparison with the cases shown in Figs. 7(a)–(f).

Here, the width of the minor loops decreases with the increase of temperature (See Ref. (7) for details of the width of the minor loops at room temperature.). For example, in the experiments, the width of the minor loop at room temperature (300°C) is about 16.4 (13.4) A/m at f_c = 1 kHz as shown in Fig. 7(a) (Fig. 7(b)). Here, the area of the minor loop depends on the iron loss caused by the minor loop. For example, in our experiments, the area of the minor loop at room temperature (300°C) shown in Fig. 7(a) (Fig. 7(b)) corresponds to 75.7 (55.5) mJ/m^3. Therefore, the area of the minor loop at high temperatures is smaller than that at room temperature because the width of the minor loops becomes narrow at high temperatures. In other words, the iron loss caused by the minor loop at high temperatures is smaller than that at room temperature. Here, as in the sinusoidal excitation tests, it is thought that due to thermal fluctuation the hysteresis losses decrease and due to the increase of electrical resistivity the classical eddy current losses decrease in the minor loops. The ratio between hysteresis and eddy current losses in the minor loops will be examined in a future presentation.

In addition, the area of the major loop in hysteresis loops under PWM inverter excitation at 300°C is smaller than that at room temperature as in the sinusoidal excitation tests shown in Fig. 4(a). We found that the temperature dependency of iron loss properties is related not only to major loop but also to minor loops. Therefore, η at 300°C is smaller than that at room temperature.

Recently, Y. Takeda *et al*. have shown that by using numerical simulations, the loss repartition between the hysteresis and eddy current losses can be obtained [32]. In addition, we have demonstrated the loss repartition in the minor loops by using the play model with the Cauer circuit [33]. Therefore, based on these results, it will be possible to estimate the loss repartition between the hysteresis and eddy current losses and between fundamental and higher harmonic components not only in the major loop but also in the minor loops at high temperatures by using our numerical simulations.

In our study, we realize the expression of hysteretic properties under inverter and sinusoidal excitations at wide range of temperature by numerical simulations. Therefore, based on our results, it is expected that we can achieve the highly accurate simulation in the PWM inverter- and sinusoidal-fed motor under a wide range of ambient temperatures.

5. Conclusions

Through the experiments and numerical simulations, this study investigated iron loss and hysteretic properties of the electrical steel sheet excited by PWM inverter under a wide range of ambient temperatures. The iron losses under sinusoidal and inverter excitations decreased with the increase of temperature. Here, it was thought that the classical eddy current loss decreased with the increase of electrical resistivity and the hysteresis loss decreased due to thermal fluctuations at high temperatures. We experimentally revealed for the first time that the temperature dependency of iron losses was related not only to a major loop but also to minor loops. Therefore, the rate of increase of iron loss at high temperatures became small in comparison with that at room temperature.

In our study, we also realized the expression of hysteretic properties of the inverter- and sinusoidal-fed ring tests at room temperature and 300°C by numerical simulations. In particular, we numerically represented the minor loop of the magnetic hysteretic phenomena by using the play model with the Cauer circuit at high temperatures. By using our numerical simulations, it will be possible to estimate the loss repartition between the hysteresis and eddy current losses and between fundamental and higher harmonic components not only in the major loop but also in the minor loops at high temperatures. Based on our numerical results, it is expected that we can achieve the highly accurate simulation in the PWM inverter- and sinusoidal-fed motor under a wide range of ambient temperatures. Therefore, our investigation of temperature dependency of iron loss characteristics in the inverter-excited magnetic core will be keys to designing the high efficiency motor drive system under a wide range of ambient temperatures.

In order to understand magnetic properties at high temperatures, further numerical and experimental studies are necessary under a wider range of temperatures. In addition, future work will incorporate improvement and extension of the numerical model to obtain predictions of magnetic properties at high temperatures. Namely, the parameter variation for thermal fluctuations suggests that a more fundamental modelling approach is required. Furthermore, in future research, the iron loss reduction of the motor core will be addressed,

since the long-term goal of the project is to derive guidelines for optimal high-temperature drive system, based on more enhanced numerical models.

Acknowledgment

This work was partly supported by the JSPS KAKENHI ♯16H07320 and the Ministry of Education, Culture, Sports, Science and Technology Program, Japan, for private universities.

References

(1) L. Burdet: "Active magnetic bearing design and characterization for high temperature applications", Ph.D. dissertation, Citeseer (2006)
(2) T.D. Kefalas and A.G. Kladas: "Thermal investigation of permanent-magnet synchronous motor for aerospace applications", *IEEE Trans. on Industrial Electronics*, Vol.61, No.8, pp.4404–4411 (2014)
(3) A. Yao, T. Sugimoto, S. Odawara, and K. Fujisaki: "Core losses of a permanent magnet synchronous motor with an amorphous stator core under inverter and sinusoidal excitations", *AIP Advances*, Vol.8, No.5, p.056804 (2017)
(4) A. Boglietti, P. Ferraris, M. Lazzari, and M. Pastorelli: "Influence of modulation techniques on iron losses with single phase dc/ac converters", *IEEE Transactions on Magnetics*, Vol.32, No.5, pp.4884–4886 (1996)
(5) A. Boglietti, P. Ferraris, M. Lazzari, and F. Profumo: "Iron losses in magnetic materials with six-step and PWM inverter supply (induction motors)", *IEEE Transactions on Magnetics*, Vol.27, No.6, pp.5334–5336 (1991)
(6) A. Boglietti, P. Ferraris, M. Lazzari, and M. Pastorelli: "Change of the iron losses with the switching supply frequency in soft magnetic materials supplied by PWM inverter", *IEEE Transactions on Magnetics*, Vol.31, No.6, pp.4250–4252 (1995)
(7) M. Kawabe, T. Nomiyama, A. Shiozaki, H. Kaihara, N. Takahashi, and M. Nakano: "Behavior of minor loop and iron loss under constant voltage type PWM inverter excitation", *IEEE Transactions on Magnetics*, Vol.48, No.11, pp.3458–3461 (2012)
(8) K. Fujisaki and S. Liu: "Magnetic hysteresis curve influenced by power-semiconductor characteristics in pulse-width-modulation inverter", *Journal of Applied Physics*, Vol.115, No.17, p.17A321 (2014)
(9) S. Odawara, K. Fujisaki, and F. Ikeda: "Proposing a numerical method for evaluating the effects of both magnetic properties and power semiconductor properties under inverter excitation", *IEEE Transactions on Magnetics*, Vol.50, No.11, pp.1–4 (2014)
(10) T. Taitoda, Y. Takahashi, and K. Fujiwara: "Iron loss estimation method for a general hysteresis loop with minor loops", *IEEE Transactions on Magnetics*, Vol.51, No.11, pp.1–4 (2015)
(11) A. Yao, K. Tsukada, S. Odawara, K. Fujisaki, Y. Shindo, N. Yoshikawa, and T. Yoshitake: "PWM inverter-excited iron loss characteristics of a reactor core", *AIP Advances*, Vol.7, No.5, p.056618 (2017)
(12) M. Noh, M. Gi, D. Kim, Y. Park, J. Lee, and J. Kim: "Measurements of magnetic properties of electromagnetic actuator in high-temperature environment", *Journal of Magnetics*, Vol.20, No.1, pp.86–90 (2015)
(13) M. Noh, M. Gi, D. Kim, Y.-W. Park, J. Lee, and J.-W. Kim: "Modeling and validation of high-temperature electromagnetic actuator", *IEEE Transactions on Magnetics*, Vol.51, No.11, pp.1–4 (2015)
(14) B. Ahmadi, F. Mazaleyrat, G. Chaplier, V. Loyau, and M. LoBue: "Enhancement of medium frequency hysteresis loop measurements over a wide temperature range", *IEEE Transactions on Magnetics*, Vol.52, No.7, pp.1–4 (2016)
(15) N. Takahashi, M. Morishita, D. Miyagi, and M. Nakano: "Examination of magnetic properties of magnetic materials at high temperature using a ring specimen", *IEEE Transactions on Magnetics*, Vol.46, No.2, pp.548–551 (2010)
(16) S. Bobbio, G. Milano, C. Serpico, and C. Visone: "Models of magnetic hysteresis based on play and stop hysterons", *IEEE Transactions on magnetics*, Vol.33, No.6, pp.4417–4426 (1997)
(17) T. Matsuo and M. Shimasaki: "An identification method of play model with input-dependent shape function", *IEEE Transactions on Magnetics*, Vol.41, No.10, pp.3112–3114 (2005)
(18) J. Kitao, K. Hashimoto, Y. Takahashi, K. Fujiwara, Y. Ishihara, A. Ahagon, and T. Matsuo: "Magnetic field analysis of ring core taking account of hysteretic property using play model", *IEEE Transactions on Magnetics*, Vol.48, No.11, pp.3375–3378 (2012)
(19) J.H. Krah: "Optimum discretization of a physical cauer circuit", *IEEE Transactions on Magnetics*, Vol.41, No.5, pp.1444–1447 (2005)
(20) Y. Shindo and O. Noro: "Simple circuit simulation models for eddy current in magnetic sheets and wires", *IEEJ Transactions on Fundamentals and Materials*, Vol.134, No.4, pp.173–181 (2014)
(21) Y. Shindo, T. Miyazaki, and T. Matsuo: "Cauer circuit representation of the homogenized eddy-current field based on the legendre expansion for a magnetic sheet", *IEEE Transactions on Magnetics*, Vol.52, No.3, pp.1–4 (2016)
(22) S. Odawara, K. Fujisaki, T. Matsuo, and Y. Shindo: "Evaluation of magnetic properties considering semiconductor properties by using numerical technique coupling inverter circuit analysis to magnetic analysis (in japanese)", *IEEJ Trans. IA*, Vol.135, No.12, pp.1191–1198 (2014)
(23) T. Miyazaki, T. Mifune, T. Matsuo, Y. Shindo, Y. Takahashi, and K. Fujiwara: "Equivalent circuit modeling of dynamic hysteretic property of silicon steel under pulse width modulation excitation", *Journal of Applied Physics*, Vol.117, No.17, p.17D110 (2015)
(24) K. Fujisaki and A. Yao: "Magnetic multi-scale model for local eddy current flow in complex materials with insulated conductive particles", *IEEE Transactions on Magnetics* (2017)
(25) A. Yao, A. Adachi, and K. Fujisaki: "Iron loss characteristics of electric motor in high-temperature environment", in 2017 IEEE International Electric Machines and Drives Conference (IEMDC). IEEE, pp.1–7 (2017)
(26) A. Yao and K. Fujisaki: "Iron loss characteristics under pwm inverter excitation at high ambient temperatures", in The 11th International Symposium on Linear Drives for Industry Applications (LDIA2017). IEEJ, pp.1–3 (2017)
(27) Non-oriented electrical steel sheets (in Japanese), Nippon Steel Corporation (2004)
(28) Special committee of silicon steel sheet: "Temperature characteristics of silicon steel sheet (in Japanese)", *The journal of the Institute of Electrical Engineers of Japan*, Vol.18, No.4, pp.289–296 (1954)
(29) D. Singh, P. Rasilo, F. Martin, A. Belahcen, and A. Arkkio: "Effect of mechanical stress on excess loss of electrical steel sheets", *IEEE Transactions on Magnetics*, Vol.51, No.11, pp.1–4 (2015)
(30) To understand electrical steel sheets (in Japanese), Nippon Steel and Sumitomo Metal Corporation (2012)
(31) Y. Shindo: "Equivalent circuit representation of electric power and electrical equipment (in japanese)", *IEEJ Journal*, Vol.137, No.8, pp.534–537 (2017)
(32) Y. Takeda, Y. Takahashi, K. Fujiwara, A. Ahagon, and T. Matsuo: "Iron loss estimation method for rotating machines taking account of hysteretic property", *IEEE Transactions on Magnetics*, Vol.51, No.3, pp.1–4 (2015)
(33) S. Odawara and K. Fujisaki: "Influence rate of semiconductor on-voltage in inverter circuit on iron loss inside a non-oriented electrical-steel-sheet", *IEEE Transactions on Magnetics (accepted)*

Appendix

1. Waveforms of Voltage and Magnetic Flux Density

app. Fig. 1 shows waveforms of the induced voltage and magnetic flux density in NO ring excited by PWM inverter at room temperature and f_c = 1 kHz. Here, the trace of

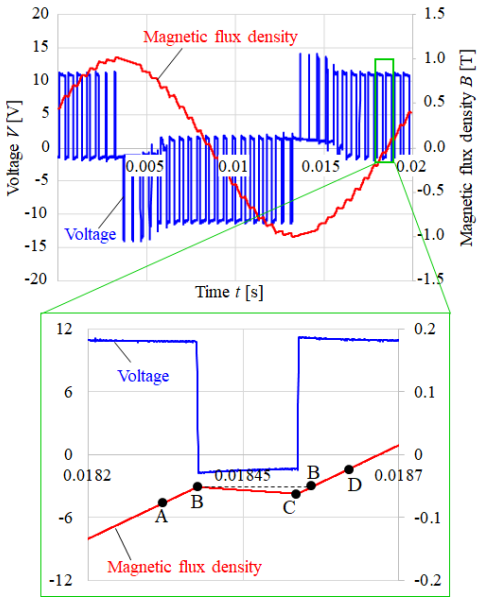

app. Fig. 1. Waveforms of induced voltage and magnetic flux density

A→B→C→B→D in the minor loop shown in Fig. 7(a) corresponds to that of A→B→C→B→D in waveforms of magnetic flux density. The area surrounded by the minor loop (B→C→B) means a part of iron losses caused by the PWM voltage. In other words, when the area surrounded by the minor loop increases, whole loss caused by the PWM voltage increases.

Atsushi Yao (Member) received Ph.D. from Kyoto University in 2015. He was a postdoctoral researcher at Kyoto University and Toyota Technological Institute from 2015 to 2016 and 2016 to 2018, respectively. He is currently an assistant professor at Toyama Prefectural University. He is a member of IEEJ, JSAP, IEICE, and so on. His research interests are including applications and control of nonlinear dynamics in micro- and nano-system and power electronics.

Shunya Odawara (Member) received B. of Eng., M.Eng., and Dr.Eng. Degrees from Saga University, Saga, Japan, in 2009, 2010, and 2013, respectively. From 2013, he was in Toyota Technological Institute, Aichi, Japan as postdoctoral researcher. Now he is in Kitami Institute of Technology, Hokkaido, Japan as research associate from 2017. His current research theme is loss characteristics evaluation by inverter excitation taking account of magnetic property and semiconductor property.

Keisuke Fujisaki (Senior Member) received the B.Eng., M.Eng., and Dr.Eng. degrees in electronics engineering from the Faculty of Engineering, The University of Tokyo, Tokyo, Japan, in 1981, 1983, and 1986, respectively. From 1986 to 1991, he conducted research on electromagnetic force applications to steel-making plants at the Ohita Works, Nippon Steel Corporation. From 1991 to 2010, he was a chief researcher in the Technical Development Bureau, Nippon Steel Corporation, Futtsu, Japan. Since 2010, he was a professor of Toyota Technological Institute. His current scientific interests are magnetic multi-scale, electromagnetic multi-physics, high efficient motor drive system, electrical motor, and power electronics. In 2002–2003, he was a Visiting Professor at Ohita University. In 2003–2009, he was a Visiting Professor at Tohoku University. Dr. Fujisaki received the Outstanding Prize Paper Award at the Metal Industry Committee sessions of the 2002 IEEE Industry Applications Society Annual Meeting.